Multi-Dimensional Simulation of n-Heptane Combustion under HCCI Engine Condition Using Detailed Chemical Kinetics

Y.Bakhshan*
Assistant Professor
Department of Mechanical Engineering
University of Hormozgan
Ybakhshan@yahoo.com

A.R.Tarahomi
MSc. Student
Department of Mechanical Engineering
University of Hormozgan
a.tarahomi@yahoo.com

Corresponding Author*
Received: Dec. 18,2010
Accepted in revised form: Feb. 14,2011

Abstract

In this study, an in-house multi-dimensional code has been developed which simulates the combustion of n-heptane in a Homogeneous Charge Compression Ignition (HCCI) engine. It couples the flow field computations with detailed chemical kinetic scheme which involves the multi-reactions equations. A chemical kinetic scheme solver has been developed and coupled for solving the chemical reactions and calculation of heat release. The effect of parameters such as, initial temperature, initial pressure, compression ratio and equivalence ratio on the combustion characteristics of a n-heptane fuelled HCCI engine have been studied. The chemical kinetic scheme used here, consists of 27 elementary reactions and 26 species which involves the reactions required for calculation of NO_x also. The results show good agreement with available experimental data.

Keywords: *HCCI, Multi-dimensional, Detailed chemical kinetic, n-heptane, Simulation*

1- Introduction

In HCCI mode, a mixture of air and fuel is compressed, with increasing the gas temperature and pressure so the auto-ignition of the fuel occurs. The advantage of this process is that the combustion occurs simultaneously in the entire combustion chamber under lean conditions. The maximum combustion temperatures are thus reduced to levels below the NOx formation threshold. Due to the nearly homogeneous and lean mixture, soot forming fuel-rich combustion is also avoided. Homogeneous Charge Compression Ignition (HCCI) engines are considered to be a new generation of internal combustion engines that operate on the basis of auto-ignition and provide a higher thermal efficiency and a lower exhaust pollutant compared to the present classic versions and are perceived as an engine for future power trains which will provide improved fuel efficiency and lower emissions. Initial papers [1-2] recognized the basic characteristics of HCCI that have been validated many times and in this engine, ignition occurs at many points simultaneously, with no flame propagation and combustion is described as very smooth with very low cyclic variation. Noguchi et al. [2] conducted a spectroscopic study of HCCI combustion and many radicals were observed. In contrast, with spark-ignited (SI) combustion all radicals appear at the same time, spatially distributed through the flame front. Najt and Foster [3] were first to run a four-stroke engine in HCCI mode and they also analyzed the process, considering that HCCI is controlled by chemical kinetics. They used a simplified chemical kinetics model to predict heat release as a function of pressure, temperature, and species concentrations in the cylinder. HCCI has several problems that have limited its commercialization, specifically it is very difficult to control the initiation and rate of combustion over the required speed and load range of these engines [4]. This is important at higher loads where very rapid pressure rise and knock are limiting. HCCI engines also operate at lower combustion temperatures, so more unburned hydrocarbons (UHC) and CO emissions are generated than in traditional engines and some of these disadvantages may be reduced or eliminated by operating these engines in “hybrid mode,” where the engine operates in HCCI mode at low power and in spark-ignited mode [5], or diesel mode [6], at high power. This hybrid mode takes advantage of high efficiency and low NOx and particulate matter emissions of HCCI engines at low power conditions. With increasing prediction ability of engine simulation tools, engine design aided by relatively low cost CFD modeling is becoming more popular in industries. In an effort to include the best representation of both fluid flow and chemical kinetics, attempts have been made to use three-dimensional CFD models coupled directly with chemical kinetics to study compression ignition under HCCI like-conditions. Agarwal and Assanis [7] reported on the coupling of a detailed chemical kinetic mechanism for natural gas ignition (22 species and 104 elementary reactions) with the multi-dimensional reacting flow code and explored the auto-ignition of natural gas injected in a quiescent chamber under diesel like conditions. Kong et al. [8] proposed a similar approach up to the point of ignition, while after ignition they introduced a reaction rate incorporating the effects of both chemical kinetics and turbulent mixing through characteristic timescales. Hong et al. [9] proposed a more computationally demanding model to simultaneously account for the effects of detailed chemistry and mixing on ignition delay within the KIVA-3V CFD code. A multi-dimensional model (the coupled model of Star-CD and CHEMKIN) was applied to investigate the combustion and emission formation of dimethyl ether (DME) and methanol dual fuel HCCI engine by Yao et al. [10]. In this study, a multi-dimensional CFD code has been developed which considers the coupling of flow field computations with a detailed chemical kinetic scheme. A chemical kinetic scheme solver has been developed and coupled for solving the chemical reactions and calculation of heat release from fuel in each control volume considered in flow field. The chemical kinetic scheme used here, consists of 26 elementary reactions and 27 species which involves the reactions required for calculation of NO_X also.

2- Model Formulation

Since detailed chemical kinetics has been used to simulate fuel oxidation, a chemical kinetic scheme solver has been developed and integrated into our multi-dimensional code for calculating the species concentrations during simulation. The convection and diffusion transport between different computational cells are modeled and the RNG k–ε turbulence model has been applied. The equations of motion for the unsteady, turbulent and chemically reactive flow are governed by the conservation of mass, momentum and energy as below;

$$\frac{\partial \rho_m}{\partial t} = \nabla \cdot (\rho_m \mathbf{u}) = \nabla \cdot [\rho D \nabla (\frac{\rho_m}{\rho})] + \dot{\rho}_m^{chem} \quad (1)$$

$$\frac{\partial \rho}{\partial t} = \nabla \cdot (\rho \mathbf{u}) = 0 \quad (2)$$

$$\frac{\partial (\rho \mathbf{u})}{\partial t} + \nabla \cdot (\rho \mathbf{u}\mathbf{u}) = -\frac{1}{a^2}\nabla p - A_0 \nabla (\frac{2}{3}\rho\kappa) + \nabla \cdot \bar{\sigma} + \rho \mathbf{g} \quad (3)$$

$$\frac{\partial (\rho I)}{\partial t} + \nabla \cdot (\rho \mathbf{u} I) = -p\nabla \cdot \mathbf{u} + (1 - A_0)\bar{\sigma} : (\nabla \mathbf{u}) - \nabla \cdot \mathbf{J} + A_0 \rho\varepsilon + \dot{Q}^{chem} \quad (4)$$

where ρm is the mass density of species , m is the total number of species, ρ is the mass density of the mixture, u is the flow velocity vector, D is mass diffusivity, I is specific internal energy, p is pressure, J is the heat flux vector accounting for contributions due to heat conduction and enthalpy diffusion, ε is the dissipation rate of turbulent kinetic energy, $\dot{\rho}_m^{chem}$ is the rate of change of species density due to chemical reactions, and $\dot{Q}^{chem}$ is the chemical heat release rate. $\dot{\rho}_m^{chem}$ and $\dot{Q}^{chem}$ are the chemistry source terms modeled by the kinetic equation. The RNG k-ε equations used for turbulent modeling are:

$$\frac{\partial (\rho\kappa)}{\partial t} + \nabla \cdot (\rho \mathbf{u}\kappa) = -\frac{2}{3}\rho\kappa\nabla \cdot \mathbf{u} + \bar{\sigma} : \nabla \mathbf{u} + \nabla \cdot [(\frac{\mu}{\mathrm{Pr}_\kappa})\nabla\kappa] - \rho\varepsilon \quad (5)$$

$$\frac{\partial (\rho\varepsilon)}{\partial t} + \nabla \cdot (\rho \mathbf{u}\varepsilon) = -(\frac{2}{3}c_{\varepsilon_1} - c_{\varepsilon_3})\rho\varepsilon\nabla \cdot \mathbf{u} + \nabla \cdot [(\frac{\mu}{\mathrm{Pr}_\varepsilon})\nabla\varepsilon] + \frac{\varepsilon}{\kappa}(c_{\varepsilon_1}\bar{\sigma} : \nabla \mathbf{u} - c_{\varepsilon_2}\rho\varepsilon) \quad (6)$$

The chemical kinetic equations are formulated as an ODE set, typically including m equations for species mass fractions Ym and one equation for gas temperature T, as below;

$$\begin{cases} \dfrac{dY_m}{dt} = \dfrac{\dot{\omega}_m W_m}{\rho} \\ \dfrac{dT}{dt} = -\dfrac{1}{\rho \bar{c}_v}\sum \dot{\omega}_m W_m I_m \end{cases} \quad (7)$$

Where $\dot{\omega}_m$ is the production/consumption rate of species m, W_m and I_m are the molecular weight and specific internal energy of species m, respectively, and $\bar{c}_v$ is the constant volume specific heat of the gas mixture. Using Eq. (7), the chemistry source terms of Eq. (1) and Eq. (4) can be written as below;

$$\dot{\rho}_m^{chem} = \rho \frac{dY_m}{dt} \quad (8)$$

Where $\Delta h_{f_m}^0$ is the molar heat of formation of species m.

The reaction mechanism used here for n-heptane consists of 26 elementary reactions and 27 species [12]. The reactions used for calculation of NO were obtained by reducing the Gas Research Institute (GRI) NO mechanism [13] and it contains four additional species (N, NO, NO_2, N_2O) and nine reactions that describe the formation of nitric oxides. The equations (1-6) have been solved with finite volume method and for coupling of pressure and velocity, the simple algorithm has been used.For solving the stiff equation of chemical kinetic scheme, a solver (DVODE) has been applied. The flowchart is shown in Fig.2.

3- Results and DIScussions

The Ford Lion HCCI engine specification used here and its data are shown in Table1.

Table 1. Engine Specifications [14]

Engine	Specification
Bore	81 mm
Stroke	88 mm
Displaced Volume	453.46 cm^3
Clearance Volume	27.82 cm^3
Compression Ratio	17.3 : 1

The calculation was carried out from IVC (-143º ATDC) to EVO (130º ATDC) and chemical kinetic calculations are invoked in a cell only when its temperature exceeds cut-off temperature. The boundaries of the mesh used in the calculation were the top of the piston, the generated dynamic mesh for inner circumferential surface of the cylinder, and the other side of the cylinder as shown in Fig.1.

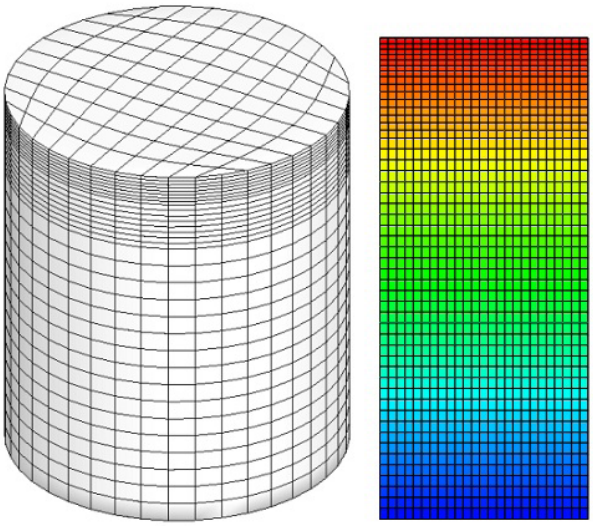

Fig 1. 2D and 3D meshes used in modeling

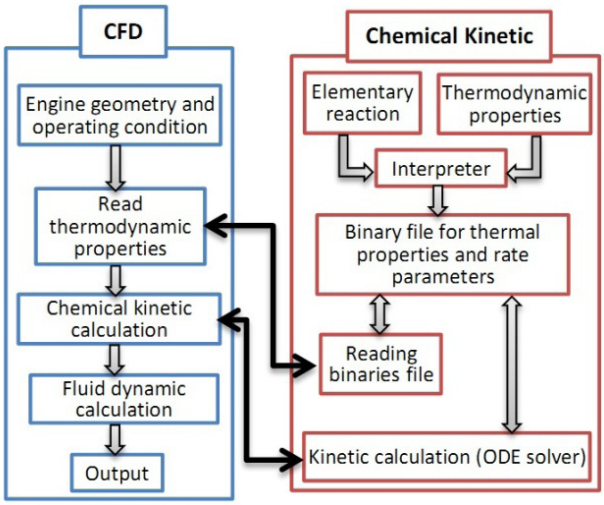

Fig 2. Flowchart of developed program

For validation of simulation results, the available experimental data for a CFR engine [15] which its specifications are shown in table2, has been used. Also the operating conditions on base engine are shown in table 3.

Table 2. CFR Engine Specifications [15]

Bore	82.55 mm
Stroke	114.3 mm
Displaced Volume	611.7 cm^3
Compression Ratio	4.6 - 16
Connecting Rod Length	254 mm
Intake valve close	-144°CA ATDC
Exhaust valve open	140°CA ATDC

The Comparison of calculation results with experimental data has been extracted for the cases of chemical kinetic schemes which include the 26-step mechanism and ERC mechanism [16] at different compression ratio.

Table 3. Base operating conditions for HCCI engine

Initial temperature	370 k
Initial pressure	1.1 bar
Compression ratio	17.3 : 1
Equivalence ratio	0.4
Engıne speed	1500 rpm

The figures 3 and 4 show the variation of in-cylinder pressure versus crank angle at different compression ratios with implementation of two chemical kinetic schemes. The equivalence ratio and engine speed in these tests are 0.4 and 900 RPM respectively. The comparison shows the good agreement between the experimental and simulation result in global, and this shows the prepared code can be used in calculation of other parameters.

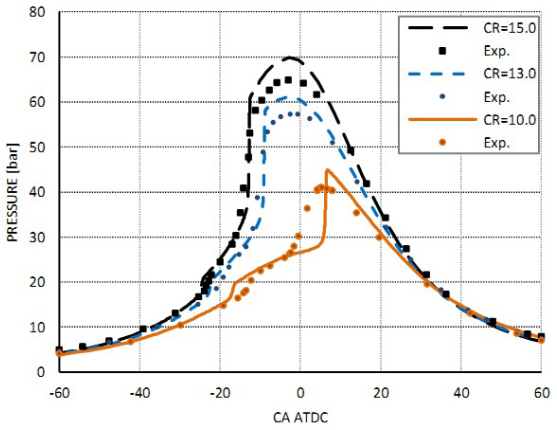

Fig 3. In-cylinder pressure vs. crank angle for different CR with ERC mechanism.

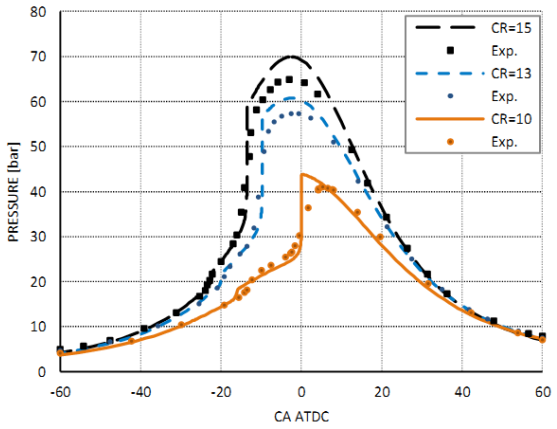

Fig 4. In-cylinder pressure vs. crank angle for different CR for 26-step mechanism.

The developed code has ability for calculation of flow field characteristics in the cylinder at operating strokes of a HCCI engine. Figure 5 shows the stream lines of in-cylinder flow at different crank angles, and the temperature contours are also shown in Figure 6. The selected crank angles are after and before top dead center and the results are in accordance with piston moving and have good agreement with predicted other global parameters.

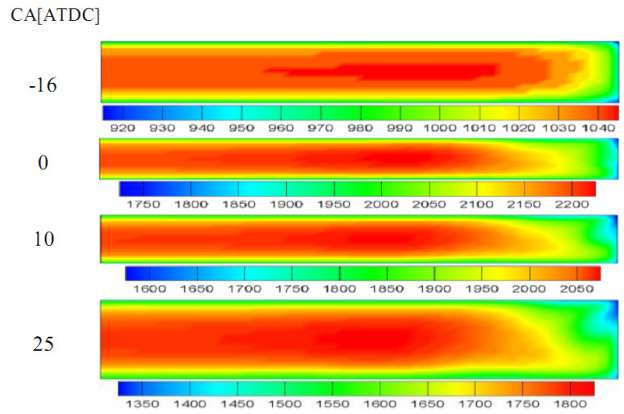

Fig 5. Temperature contours at different crank angles

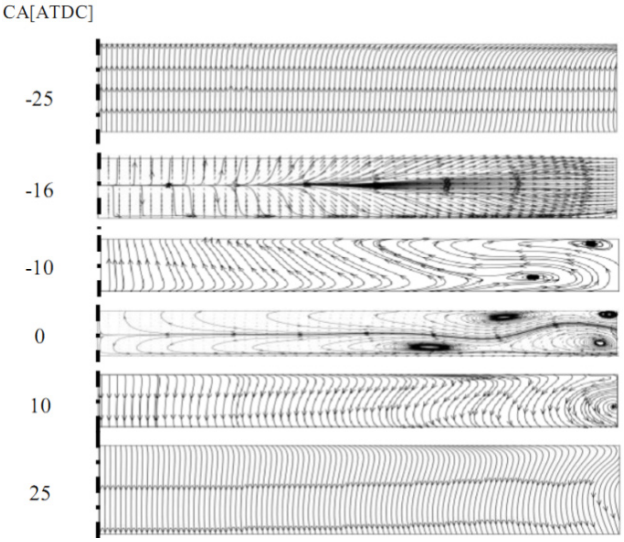

Fig 6. Stream lines of in-cylinder flow at different crank angles

After validation, the developed code has been applied for basic engine whose data are shown in table1. With considering the operating conditions of a HCCI engine, the variation of some species such as NO,NO_2,N_2O,fuel,O_2,CO2,H_2O and CO are shown in figures 7-9.

Figure 7. shows the variation of the main combustion products and reactants with crank angle. The major pollutants produced in the cylinder due to oxidation of fuel are shown in Figures 8 and 9. The variations of all species have good consistency with chemical kinetic scheme implemented in modeling in overall. It was found that the CO value increased rapidly at the start of combustion, but after the combustion completion, the oxidation of CO took more speed and its concentration would, therefore, decrease.

The nitrogen oxides (NOx) are important pollutants in internal combustion engines and the variation of nitrogen oxides (NOx) are shown in Figure9. The NO concentration increases rapidly with starting of combustion due to increasing the temperature and its value freeze after taking the maximum value, so this is compatible with extended Zeldovich mechanism applied in this modelling which considers only thermal formation of NO. Also the N_2O and NO_2 species have good prediction as shown in Figure 9. Also, with starting the combustion and rising the in-cylinder temperaure, the emission NO is produced and take it maximum value but its value is decreased a few in continous.With starting the chemical kinetics reactions(onset of combustion), the free radical (OH) is produced and increased and reached to its maximum value,but in expansion stroke is consumed.

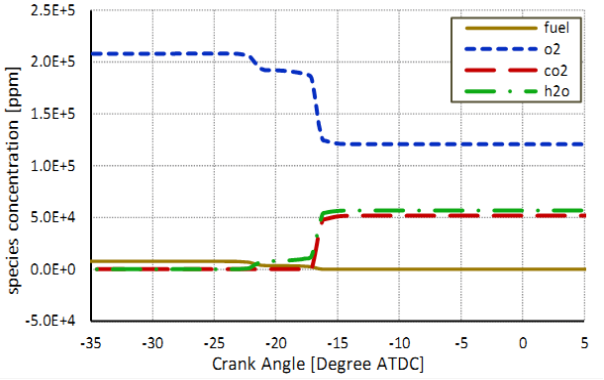

Fig 7. Fuel,O_2,CO_2,H_2O concentrations variation versus crank angle

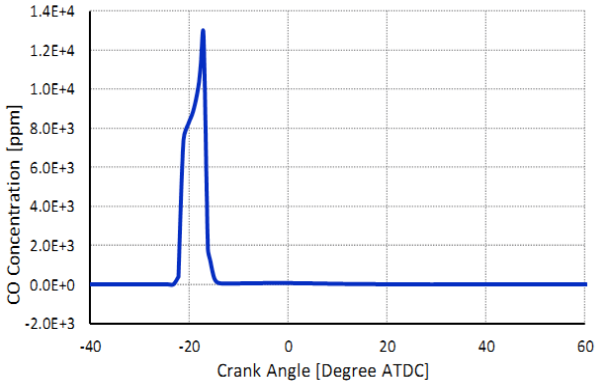

Fig 8. CO concentrations variation versus crank angle.

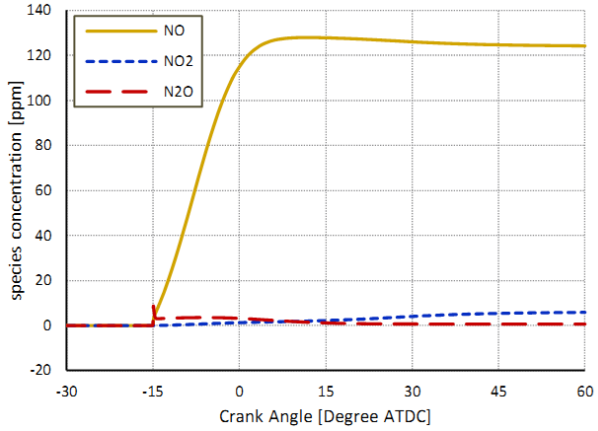

Fig 9. NO,NO_2 and N_2O concentrations variation versus crank angle.

Several parametric studies of intake charge temperature, pressure, equivalence ratio and compression ratio were carried out and these studies are shown graphically in figures 10-22.The equivalence ratio is an important operating parameter and has more effects on performance and pollutants emission in internal combustion engines. The effects of this parameter on performance and pollutants variation are shown in figures 10, 11 and 12. With increasing the equivalence ratio, the pressure and temperature dependent pollutants, such as NO increase and at the stoichiometric point, the concentration of NO take the maximum values due to higher combustion temperature at this condition. When the mixture is richer, the concentration of oxygen decreases, while the maximum temperature as well as the concentrations of NOx will decrease, whereas with leaner mixture, the maximum temperature decreases. With increasing temperature and pressure at the start of compression stroke, the pressure and temperature of in-cylinder will increase and starting of combustion shifts to earlier and this is because the increasing of temperature will start the chemical reactions and onset of combustion finally. Also with high value of initial pressure and temperature NOx increases due to increasing the maximum in-cylinder temperature.

Figure 13 shows the in-cylinder pressure variation with crank angle at different compression ratios. The pressure rising at a specific crank angle shows the start of combustion so with increasing the compression ratio, the in-cylinder temperature and pressure increases and it results in the combustion (starting the chemical reactions) starts with delay time. The cumulative heat release from fuel combustion is shown in figure 15. With increasing the compression ratio,the released energy increases and also the start of heat release is moving forward on crank angle with compression ratio variation.

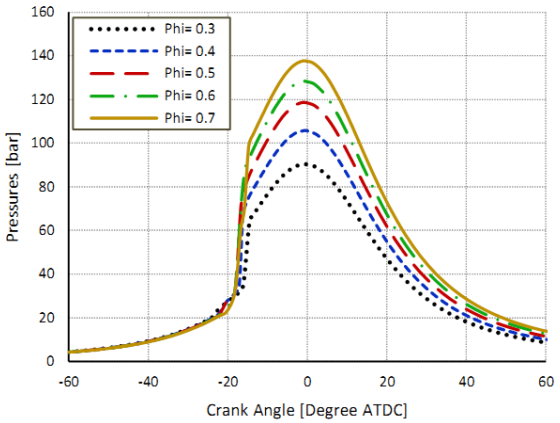

Fig 10. In-cylinder pressure vs. crank angle at different equivalence ratios.

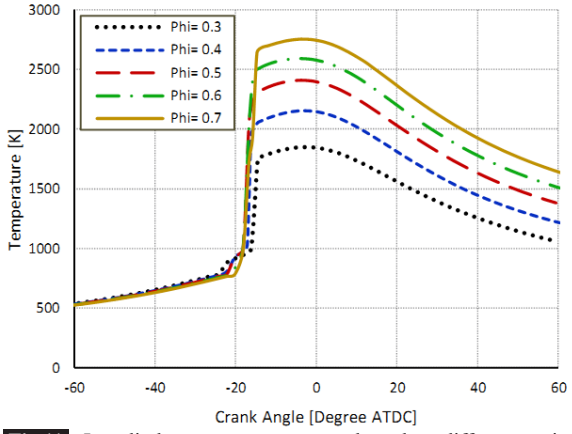

Fig 11. In-cylinder temperature vs. crank angle at different equivalence ratios.

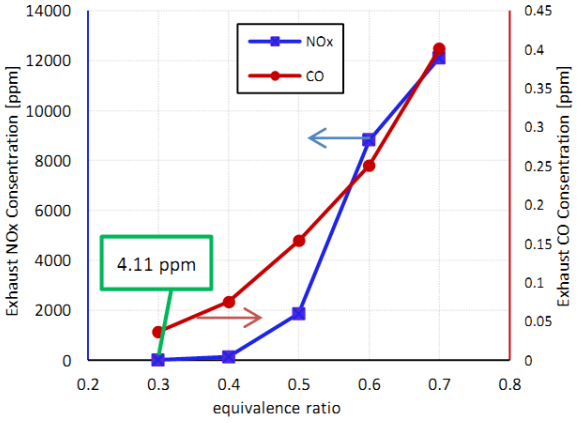

Fig 12. Effect of equivalence ratio on pollutants

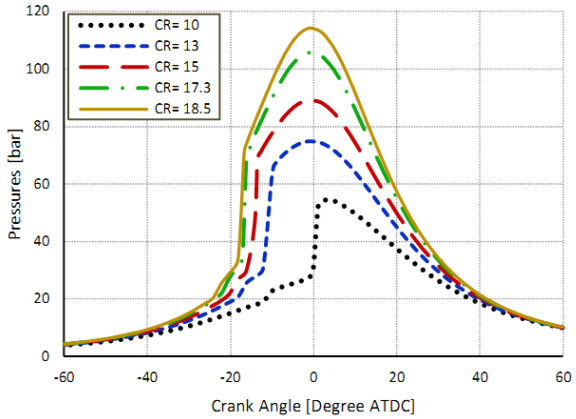

Fig 13. In-cylinder pressure vs. Crank angle at different compression ratios

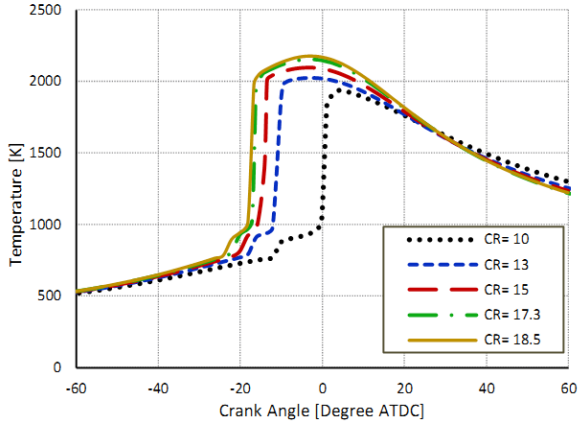

Fig 14. In-cylinder temperature versus CA at different compression ratios.

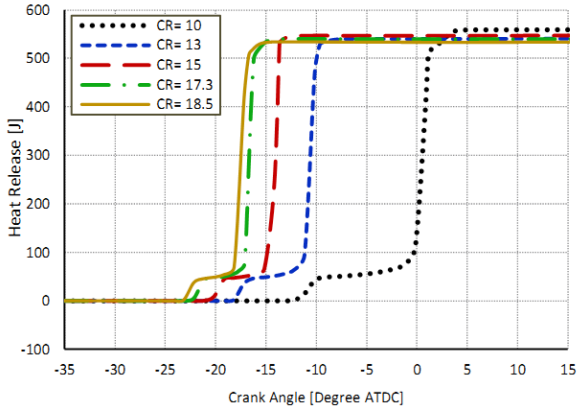

Fig 15. Cumulative heat release versus crank angle at different compression ratios.

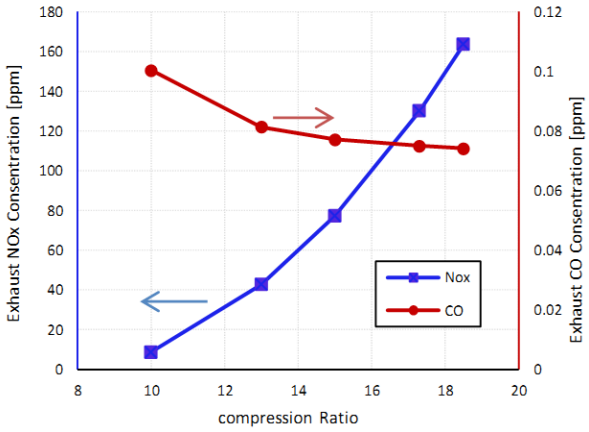

Fig 16. Effect of compression ratio on major pollutants variation

Figures 17 and 18 show the variation of in-cylinder pressure and temperature versus the crank angle at the different initial temperature (inlet temperature at the start of compression stroke).With combustion (chemical reactions) will start at later on crank angle and this is because the in-cylinder temperature is decreasing so the activation energy is not enough for starting combustion at earlier time. Also with decreasing the inlet temperature at the start of compression stroke and decaying the starting point of combustion, the most of total energy is released at the near the end of compression stroke and thus the peak pressure, temperature and fuel consumption increase more.With increasing the intake charge temperature, the peak in-cylinder temperature will take higher values but it must be notified that the fuel mass and total heat released are constant for all intake temperature and the density and volumetric efficiency will decrease, but the effect of it is less. The intake temperature effect on pollutants is shown in figure 19 and with increasing the intake temperature, the maximum value of temperature and so the pollutants are increased.

The pressure effects are similar to temperature and are shown in figures 20, 21 and 22.With increasing the intake charge pressure, the in-cylinder temperature, in-cylinder pressure and dependent pollutants are increased.

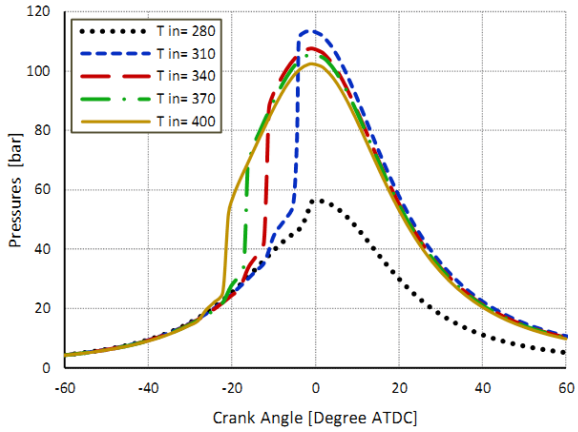

Fig 17. Effect of intake charge temperature on ignition

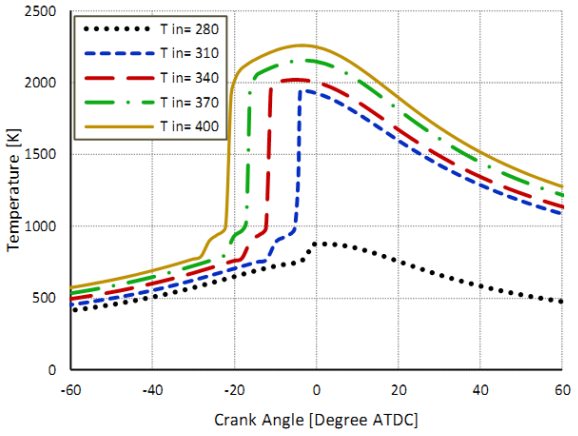

Fig 18. Variation of in-cylinder temperature with crank angle at different intake temperatures.

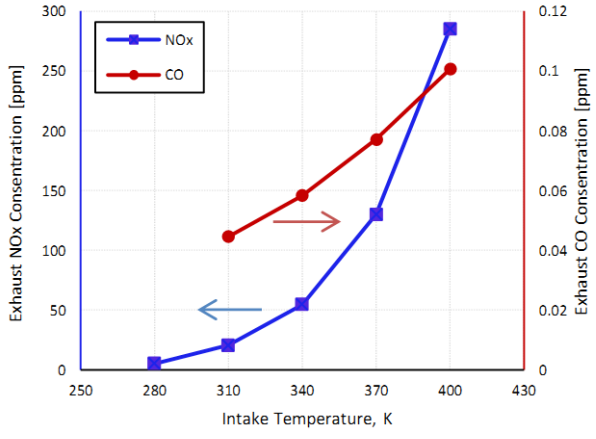

Fig 19. Variation of pollutants emission with intake temperature.

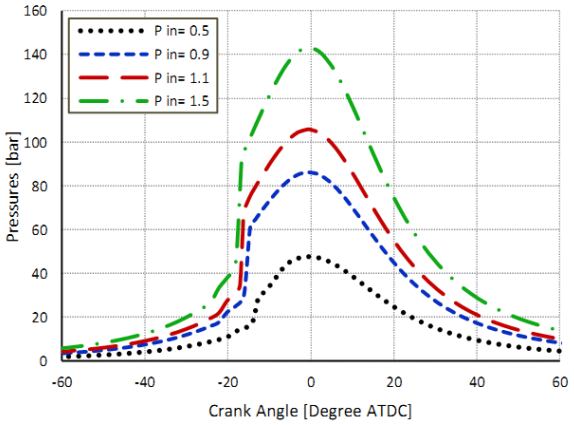

Fig 20. Effect of intake charge pressure on ignition.

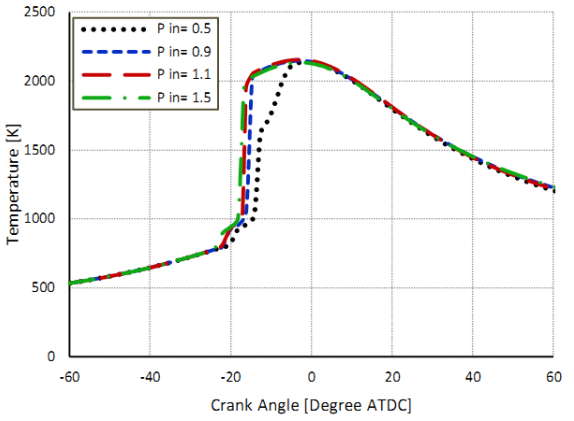

Fig 21. Effect of intake charge pressure on in-cylinder temperature

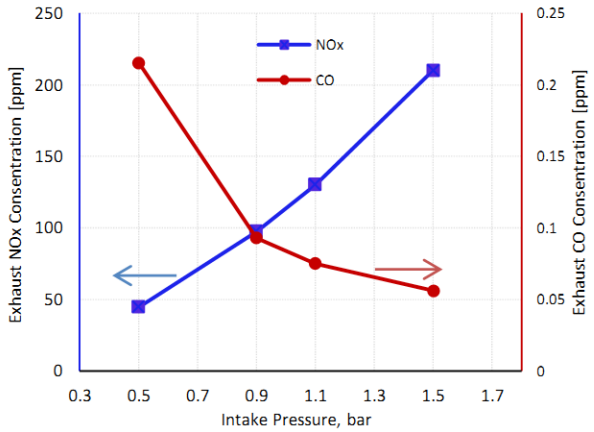

Fig 22. Effect of intake charge pressure on pollutants

4- Conclusion

An in-house multi-dimensional code has been developed which simulates the processes of a Homogeneous Charge Compression Ignition (HCCI) engine. It considers the coupling of flow field computations with a detailed chemical kinetic scheme which involves the multi-reaction equations. A chemical kinetic scheme solver has been developed and coupled for solving the chemical reactions and calculation of heat release from fuel in each control volume considered in flow field. The effect of parameters such as the swirl at the start of compression stroke, initial temperature, initial pressure, engine speed, compression ratio and equivalence ratio on the combustion characteristics and performance of a n-heptane fuelled HCCI engine have been studied.

5- Nomenclature

Latin Equation Symbols

After Top Dead Center	ATDC
molar concentration	C
Crank Angle	CA
Activation energy	E
intake valve closure	IVC
Internal energy	I
Turbulent KE, reaction rates	k
Mass	m
Cylinder gas pressure	P
Progress variable	q
Gas constant	R
Temperature	T
Velocity Vector	$\boldsymbol{u}$
Molecular Weight	W_m
Mass Fraction Species	Y

Greek Equation Symbols

Chemical production rate	$\dot{\omega}$
Density	ρ
Eddy dissipation	ε

Subscript Equation Symbols

species index	m

6. Refrences

[1] S. Onishi, S.H. Jo, K. Shoda, P.D. Jo, and S. Kato, "Active thermo-atmosphere combustion ATAC: a new combustion process for internal combustion engines," SAE Paper 790501, 1979.

[2] M. Noguchi, Y. Tanaka, T. Tanaka, and Y. Takeuchi, "A Study on Gasoline Engine Combustion by Observation of Intermediate Reactive Products During Combustion," SAE Paper 790840.

[3] P.M. Najt and D.E. Foster, "Compression-ignited homogeneous charge combustion," SAE Paper 830264, 1983.

[4] T.W. Ryan III, and T.J. Callahan, "Homogeneous Charge Compression Ignition of Diesel Fuel, " SAE Paper 961160, 1996

[5] Y. Ishibashi, and M. Asai, "Improving the Exhaust Emissions of Two-Stroke Engines by Applying the Activated Radical Concept," SAE Paper 960742, 1996.

[6] S. Kimura, O. Aoki, H. Ogawa, S. Muranaka, Y. Enomoto, "New Combustion Concept for Ultra-Clean and High-Efficiency Small DI Diesel Engines, " SAE Paper 1999-01-3681, 1999.

[7] A. Agarwal and D. N. Assanis, "Multi-dimensional modeling of natural gas ignition under compression ignition using detailed chemistry," SAE paper 980136, 1998.

[8] S. C. Kong, C. D. Marriott, and R. D. Reitz, "Modeling and Experiments of HCCI Engine Combustion Using Detailed Chemical Kinetics with Multidimensional CFD," SAE paper 2001-01-1026, 2001.

[9] S. Hong, M. Woold ridge, and D. N. Assanis, "Modeling of Chemical and Mixing Effects on Methane Auto ignition Under Direct Injection stratified Charge Conditions, " Proceeding of the 29th International Symposium on Combustion, 2002.

[10] M.F. Yao, C. Huang, Z.L. Zheng, "Multi-dimensional numerical simulation on dimethyl ether/methanol dual fuel HCCI engine combustion and emission processes, " Energy Fuel 2007;21(2):812–21.

[11] R. J. Kee, F. M. Rupley, and J. A. Miller, "CHEMKIN-II: A FORTRAN Chemical Kinetics Package for the Analyses of Gas Phase Chemical Kinetics," Sandia Report, SAND 89-8009, 1989.

[12] F. Maroteaux and L. Noel, "Development of a reduced n-heptane oxidation mechanism for HCCI combustion modeling," Combustion and Flame, vol. 146, pp. 246–267, 2006.

[13] G. P. Smith et al. (2010, June) http://www.me.berkeley.edu/gri mech.

[14] T. M. Foong, "Setup of Common-Rail Small-Bore High-Speed Direct-Injection Diesel Engines for Biodiesel Combustion Studies," M.Sc Thesis: University of Illinois. Urbana. 2009.

[15] H. Guo, W. S. Neill, and W. Chippior, "An Experimental and and Modeling Study of HCCI Combustion Using n -Heptane," Engineering for Gas Turbines and Power, vol. 132, 2010.

[16] A. Patel, S. C. Kong, and R. D. Reitz, "Development and validation of a reduced reaction mechanism for HCCI engine simulations," SAE Paper 2004-01-0558, 2004.

[17] S.H. Mansouri, and Y. Bakhshan, "The k-epsilon Turbulence modelling of heat transfer and Combustion processes in a Texaco Controlled Combustion Stratified Charge Engine", Journal of Automobile Engineering, ImechE, PartD, Vol 214, UK, 2000.

[18] S.H. Mansouri, and Y. Bakhshan, "Studies of NOx, CO, Soot formation and oxidation from direct-injection Stratified-Charge Engine Using k-epsilon Turbulence Model," Journal of Automobile Engineering, ImechE, PartD, Vol 215,UK.,2001.

[19] Y. Bakhshan, A.H.shadaei, " Quasi-Dimensional Modelling of a CNG fueled HCCI engine Combustion Using Detailed Chemical Kinetic " Accepted to Journal of Applied fluid mechanics (JAFM), Iran, 2011.